IEEE Access
Multidisciplinary | Rapid Review | Open Access Journal

Received September 23, 2021, accepted October 7, 2021, date of publication October 13, 2021, date of current version October 21, 2021.

Digital Object Identifier 10.1109/ACCESS.2021.3119533

Toward High Resolution 3D Printing of Shape-Conformable Batteries via Vat Photopolymerization: Review and Perspective

ALEXIS MAUREL[1,2], ANA C. MARTINEZ[1,2], SYLVIE GRUGEON[3,4], STÉPHANE PANIER[3,5], LOIC DUPONT[3,4], PEDRO CORTES[6], CAMEROUN G. SHERRARD[7], IAN SMALL[7], SREEPRASAD T. SREENIVASAN[2], AND ERIC MACDONALD[1], (Senior Member, IEEE)

[1]Department of Mechanical Engineering, The University of Texas at El Paso, El Paso, TX 79968, USA
[2]Department of Chemistry and Biochemistry, The University of Texas at El Paso, El Paso, TX 79968, USA
[3]Laboratoire de Réactivité et de Chimie des Solides, UMR CNRS 7314, Hub de l' Énergie, Universitéde Picardie Jules Verne, 80039 Amiens Cedex, France
[4]RS2E, Réseau Français sur le Stockage Électrochimique de l' Énergie, FR CNRS 3459, 80039 Amiens Cedex, France
[5]Laboratoire des Technologies Innovantes, LTI-EA 3899, Université de Picardie Jules Verne, 80025 Amiens, France
[6]Department of Civil, Environmental, and Chemical Engineering, Youngstown State University, Youngstown, OH 44555, USA
[7]NASA Marshall Space Flight Center, Huntsville, AL 35812, USA

Corresponding authors: Alexis Maurel (amaurel@utep.edu), Ana C. Martinez (acmartinezm@utep.edu), and Eric MacDonald (emac@utep.edu)

This work was supported in part by the French Fulbright Program, and in part by The University of Texas at El Paso (UTEP) Murchison Chair.

ABSTRACT High-resolution additive manufacturing offers access to the production of intricate architectures with small features that can revolutionize the fabrication of next-generation batteries. Relegated to two-dimensional sheets, commercial lithium-ion batteries consist of stacked leaflets, which are manufactured in restricted stacked or rolled geometries. By leveraging the most recent advancements of vat photopolymerization (VPP), the next-generation of shape-conformable three-dimensional batteries can be co-designed with known application requirements and provide enhanced safety and power performance based on reduced weight and dead volume. Herein, an overview of the state of the art with perspectives towards the development of electroactive photo-polymerizable resins for the direct fabrication of complete multi-material three-dimensional batteries is presented. Different approaches are described, including the formulation of composite resin through the introduction of solid electroactive particles, soluble components or metal precursors. Finally, the impact of the thermal post-processing steps on the resulting electrochemical properties of the VPP printed battery component or device is thoroughly discussed. This study paves the way towards the manufacturing of a complete high-resolution shape conformable 3D battery via VPP with enhanced power density.

INDEX TERMS Lithium-ion battery, electrodes, 3D printing, vat photopolymerization, composite.

I. INTRODUCTION

Motivated by the increasing demand of portable electronic devices and the commercialization of electric vehicles, the last decades have witnessed the development of new energy storage systems. Lithium-ion batteries (LIB) have remained the system of choice due to the promising electrochemical performances including high energy density, power density, efficiency and long cycle life. Despite the impressive commercial growth of LIB worldwide, research challenges still remain regarding the synthesis, fabrication, electrochemical performance, and safety.

In the last few years, research dedicated to LIB has been focused on the development of unconventional three-dimensional (3D) architectures. Originally initiated from the work of Long *et al.* [1], this focus has been motivated by the capability of 3D battery architectures to provide higher active exchange surface area and enhanced lithium-ion diffusion. Such architectures improve the electrochemical performance in terms of specific capacity, areal energy density and power density [2], [3]. Many groups have attempted to develop 3D arrangements of independent battery electrodes by inducing an electrochemical growth of nanorods/micro-tubes/post arrays onto a current collector serving as substrate followed by electrochemical plating of the active material (Fig. 1) [4]–[6]. While surface irregularities were unfortunately introduced and often resulted in short circuits (while performing the intercalation of both electrodes), these pioneering studies have established a process and geometric architecture well suited to be further improved with the design and fabrication freedom of additive manufacturing (also referred to informally as 3D printing).

Unlike conventional fabrication techniques, additive manufacturing allows the development of energy storage devices

The associate editor coordinating the review of this manuscript and approving it for publication was Agustin Leobardo Herrera-May.

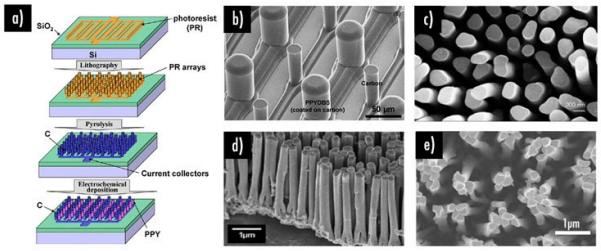

FIGURE 1. (a) Preparation of a carbon/polypyrrole 3D battery [4]; (b) scanning electron microscopy (SEM) image of carbon/dodecylbenzenesulfonatedoped polypyrrole post arrays [4]; (c) SEM micrograph of electrodeposited aluminum nanorods [5]; (d) SEM cross-sectional view of copper-nanopillars grown on a copper substrate [6]; (e) SEM top view of nickel-nanopillars grown on a nickel substrate [6].

such as LIB based on a layer-by-layer material deposition fashion with the possibility of producing highly complex 3D geometries such as intricated gyroid design (Fig. 2a). Besides the capability of manufacturing unique 3D batteries architectures for power applications, 3D printing also opens up the implementation of shape-conformable [7], [8] or structural [9] energy storage devices by reducing dead volume and weight within the final object (Fig. 2b). This represents a promising solution for producing lightweight portable devices and transportation structures including the aerospace and aeronautical sector.

Most of the early studies reported in literature relating to additively manufactured energy storage structures are focused on material extrusion (ME) due to the wide availability of inexpensive desktop printers and include research with direct ink writing [12]–[15] and fused filament fabrication [7], [8], [10], [16]–[19]. However, other additive manufacturing techniques such as vat photopolymerization (VPP), are starting to be used to construct batteries. Main advantage of VPP for battery applications is based on its improved resolution ranging from 100 μm down to 100 nm (Fig. 3). Based on the American Society for Testing and Materials, VPP includes three technologies: stereolithography using a laser to cure photoresins, digital light processing with a projected image, and two-photon polymerization (2PP) in which the intersection of two photons induces solidification. With light defining the high resolution and intricate geometric features, and a liquid feedstock providing improved surface finish, these technologies outperform in terms of resolution the less expensive thermoplastic material extrusion processes.

A summary of previous works regarding vat photopolymerization specifically employed for LIB applications is presented in this review. An overview of the different approaches employed to prepare the composite resin for the printing of electrode and electrolyte structures is discussed. Being a relatively emerging topic, an outlook of the future investigation trends and perspectives on VPP applied to LIB is comprehensively detailed.

II. VAT PHOTOPOLYMERIZATION

VPP is a process that selectively cures in a layer-by-layer fashion a vat of liquid photosensitive resin composed of a mixture of monomers, oligomers, photoinitiator, light absorbers and photosensitizers [21]. The chemistry behind the photo-polymerization process (free-radical) is rather simple: photons of a specific wavelength in the UV-range provide the required energy to the photoinitiator (Fig. 4a) so that the photocuring process propagates and builds a cross-linked polymeric network. Acrylate-based resins (containing for example poly(ethylene glycol) diacrylate (PEGDA)) are the most commonly used due to their high reactivity [20]. The process begins when the photoinitiator, for instance diphenyl (2,4,6-trimethylbenzoyl)-phosphine oxide, absorbs the photon energy and forms two free radicals. Then a radical opens a carbon-carbon bond in the PEGDA monomer and initiates a chain-reaction with available vinyl bonds until only dead-end polymer chains exist (Fig. 4b) [22], [23]. Tuning the resin properties can be achieved through the addition of a photo-absorber or a photosensitizer that respectively limit or promote the photoexcitation and curing depth.

III. VPP OF BATTERIES FROM RESINS LOADED WITH SOLID PARTICLES

Currently, no studies have reported the preparation and printability of highly loaded composite resins containing solid particles such as active materials and conductive additives to obtain composite LIB electrodes or ceramic electrolyte via VPP. Nonetheless, the formulation of composite resins containing active materials/fillers had been widely investigated (Table 1) for other applications including dentistry and electronics to confer unique properties and functionalities (including thermal stability, piezoelectricity, mechanical strength, magnetism or biocompatibility) as well as to decrease shrinkage upon polymerization. [24], [25]

As clearly stated by Tan *et al.* [24], filler loading, concentration and particle size must be thoroughly controlled to limit the viscosity of the resin, since it could obstruct the recoating process, and have a detrimental effect on the whole printability. This issue can nonetheless be overcome by slightly increasing the resin temperature during the printing [26], using smaller filler particles [27] or through the introduction of a dispersant and diluent [28]. Furthermore, when dealing with composite resin loaded with solid particles, their density must be considered, and viscosity of the resin must be thoroughly tuned to avoid filler sedimentation.

In this context, printing of a highly loaded composite resin with up to 53 vol% of alumina powder was reported by Hinczewski *et al.* [28]. In order to increase the ceramic fraction while maintaining a low viscosity and homogeneous suspension, a dispersant (azeotropic mixture of methylethylketone and ethanol 60:40 vol. ratio) and a diluent (n-butyl acryloyloxy ethyl carbamate) were introduced, while the vat temperature was tuned. The dispersant was reported to act both by electrostatic and steric repulsion by dispersing the alumina particles in a low polar organic media. Similarly, other groups have reported printing of composite resins loaded with alumina (Fig. 5a) [29, 30], but also other ceramics such as silica [31]–[33], silicon nitride [31], boron nitride-silica [34] and zirconia [35].

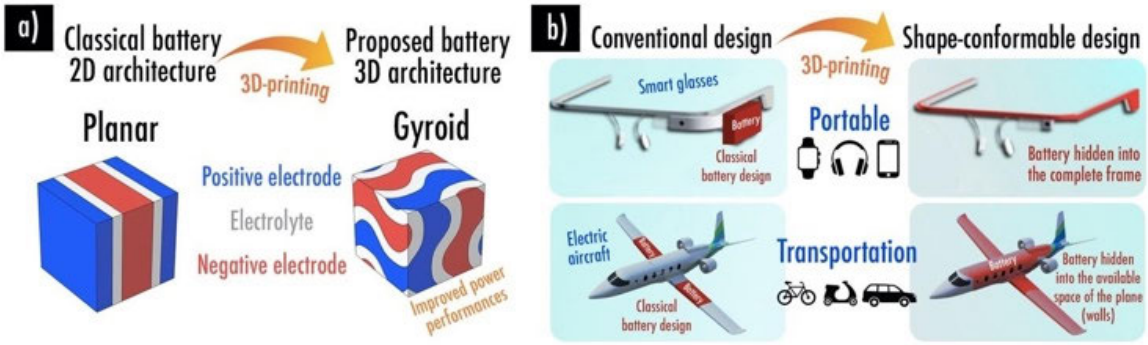

FIGURE 2. (a) Conventional 2D battery architecture and innovative 3D gyroid architecture; (b) Examples of shape-conformable batteries that can be obtained thanks to additive manufacturing [10], [11].

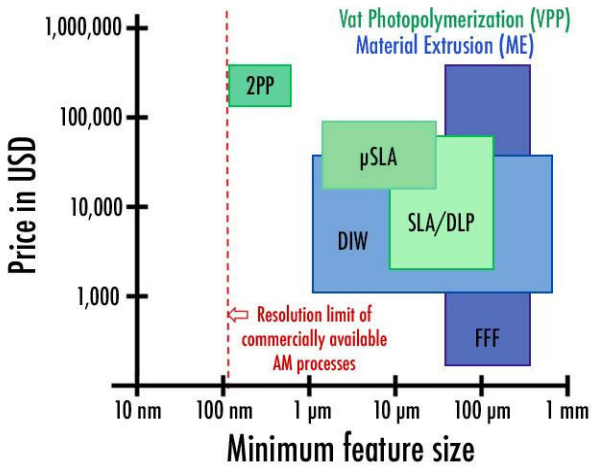

FIGURE 3. Comparison of additive manufacturing technologies in terms of resolution and capital cost. Adapted from Zhakeyev *et al.* [20]. VPP comprises 2PP, μSLA, and SLA/DLP. 2PP stands for two-photon polymerization, μSLA for micro-stereolithography, and DLP for digital light processing. ME comprises DIW and FFF. DIW stands for direct ink writing and FFF for fused filament fabrication.

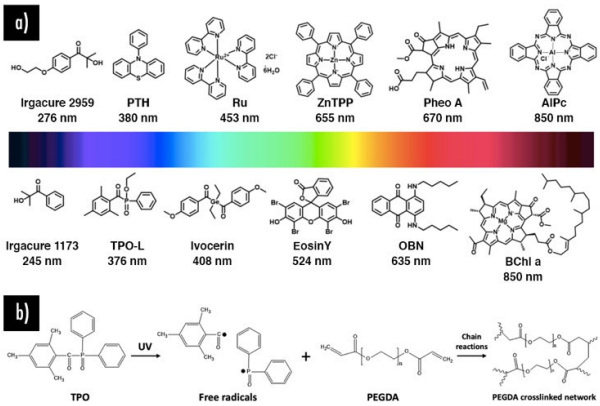

FIGURE 4. (a) List of employed photoinitiators and their respective specific wavelength [23]; (b) Schematic PEGDA photopolymerization reaction [22]. TPO stands for diphenyl (2,4,6-trimethylbenzoyl)-phosphine oxide.

It is worth mentioning that the main difficulty when considering printing a composite resin loaded with solid particles is the resulting optical properties. Filler particles must negligibly contribute to light scattering and be adequately clear to allow satisfactory curing depth (C_d). Derived from the Beer-Lambert law, C_d can be expressed as (1):

$$C_d = D_P \times ln(E_{max}/E_c) \tag{1}$$

where D_P is the penetration depth of light, E_{max} (J/m^2) the exposure, and E_c, (J/m^2) the critical minimal exposure to initiate polymerization of the photocuring resin. For a loaded resin, D_P is a function of the volume concentration of the powder, particle diameter and the refractive index difference between the UV-curable solution and the powder [28], [36].

In this framework, while the introduction of solid particles seems the most logical route to follow in order to produce LIB components, experiments are significantly limited due to the high viscosity of the composite resin as well as the considerably lower curing depth compared to traditional UV-curable resin containing only polymeric matrix and photoinitiator [37], [38]. Nevertheless, loading of resin with solid particles of electroactive materials is possible and has lately been considered for the preparation of other energy storage devices such as supercapacitors and capacitors. Park *et al.* [39] recently reported the preparation of a UV-curable composite resin with silver nanowires. Using DLP, the authors were able to print 3D hierarchical octet truss structure (Fig. 5b). After performing pyrolysis on the structure, a silver 3D array was obtained and used as a supercapacitor (Fig. 5c). Likewise, Yang *et al.* [40] reported the elaboration of 3D-printed capacitors via DLP based on the incorporation of Ag/Pb(Zr,Ti)O_3 filler particles (up to 18%vol) into the UV-curable polymer resin. In this study however, the green part (name given to the item immediately after the printing stage) was directly subjected to electrochemical testing without performing any additional thermal post-processes.

Based on these pioneering studies, no doubt that future works will demonstrate the energy storage capability of VPP printed LIB electrodes/ceramic electrolytes components containing solid particles. As thoroughly detailed hereafter, the electrochemical performances of the printed item can be evaluated at two different stages: 1) on the green part (before debinding and sintering steps); 2) on the sintered part (after these two thermal post-processing steps).

A. GREEN STATE ITEMS

The main feature of the production of functional battery components directly at the green state is that no thermal post-processing is needed as part of the manufacturing stages. The electrochemical properties of the printed green item can

TABLE 1. Formulation of composite resins loaded with solid particles reported in literature.

Solid particles	Photocurable resin	3D-printing process and parameters	Reference
α-Al_2O_3 (particle size: 0.5 µm; loading up to 53 vol%)	Monomer: di-ethoxylated bisphenol A dimethacrylate Dispersant: methylethylketone and ethanol Diluent: n-butylacryloyloxy ethyl carbamate Photoinitiator: 2,2 dimethoxy-2-phenylacetophenone	SLA Layer thickness: 200 µm	[28]
Al_2O_3	Commercial resin	DLP Layer thickness: 25 µm Radiant exposure: 130 mJ/cm^2	[29]
Al_2O_3 (particle size: 0.46 µm), **SiO_2** (2.3 µm), Si_3N_4 (0.44 µm); loading between 40 and 55 vol%	Monomer: hexane diol diacrylate (HDDA) Dispersant: unknown Photoinitiator: unknown	SLA Layer thickness: 150 µm Radiant exposure: 100 to 5200 mJ/cm^2	[31]
h-BN-SiO_2 (particle size: 1 µm; loading up to 50 vol%)	Monomers: Ethoxylated (5) Pentaerythritol tetraacrylate; polyurethane acrylate; HDDA; Dispersant: capryl alcohol Photoinitator: PEG300	DLP Layer thickness: 50 µm	[34]
ZrO_2 (particle size: 0.2 µm; loading up to 55 vol%)	Monomer: HDDA; 1,1,1-trimethylolpropane triacrylate Dispersants: KOS110; KOS163; Solsperse 17000 Photoiniator: TPO	—	[35]
Silver nanowires (50 nm in diameter and 10 µm in length; loading: 13 wt.%; for supercapacitors application)	Monomers: methacrylic acid; urethane tri-acrylate Photoinitiator: TPO	DLP Layer thickness: 30 µm Radiant exposure: 1350 µW/cm^2 Printed electrode performances: 3.01 mF/g (0.301 mF/cm^2) at scan rate of 200 mV/s	[39]
Ag/Pb(Zr,Ti)O_3 (particle size: 3 µm; up to 18 vol%)	Commercial resin	DLP Layer thickness: 20-40 µm Printed electrode performance: 65 F/g at scan rate of 20 mV/s	[40]

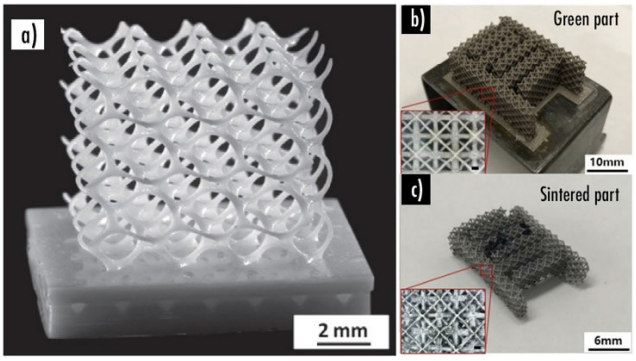

FIGURE 5. (a) Sintered alumina lattice structure [29]; (b) 3D printed octet structure obtained from a composite resin loaded with silver nanowire; (c) 3D printed octet structure after thermal post-processing [39].

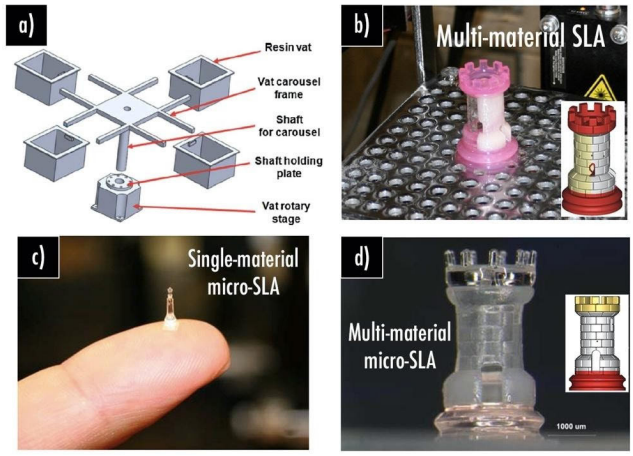

FIGURE 6. (a) Multi-material SLA option involving a rotating vat carousel system [47]; (b) 3D printed "rook" and model (inset) using a multi-material SLA option [47]; (c) Single-material fabrication of "king" chess piece via micro-SLA [48]; (d) 3D printed "rook" and model (inset) using a multi-material micro-SLA option [48].

be directly characterized after printing. Nevertheless, poor battery performances (specific capacity, energy and power density) are expected at this stage due to the presence of a high quantity of non-electroactive polymer matrix, acting as dead material, and the low porosity of the printed item. Printed electrodes are thus expected to exhibit low electrical conductivities as well as poor electrolyte impregnation, both of which will result in poor specific capacity during cycling, even at low current densities. Printed current collectors at the green state would also exhibit low electronic conductivity for the same reasons stated before. It has been previously demonstrated that the printing of infill patterns, or of lattice electrodes with open porosity, could enhance the electrodes performance at the green state by increasing the available electroactive surface area and the liquid electrolyte impregnation [41]. Another possibility would be to add a water-soluble salt into the resin that would be removed after printing simply by soaking the printed green item in a solution, thus creating an intentional porosity. It is worth mentioning that maintaining the mechanical strength of the printed electrodes and collector is a critical feature to provide robust battery parts. The investigation of conductive parts in the green state could provide sturdy structures capable of yielding superior mechanical properties than their sintered counterparts (which tend to be brittle as the strength is only conferred by the consolidation of the electroactive material).

As the printability of the complete battery in one single print (or ''one-shot'') via VPP still remains one of the main targets to achieve, it is important to note that having composite resins with the same polymeric matrix would improve the adherence between the various layers and components (electrodes, current collectors, electrolyte) in the green state. While multi-material printing options [42]–[44] had been widely commercialized for material extrusion [2], [45], or inkjet additive manufacturing processes, their counterparts for VPP are still scarce as only few attempts at the laboratory scale have been carried out over the last years. These attempts have generally resulted in an exponential decrease in the production rate. Inamdar *et al.* [46] modified a commercial SLA system and implemented the use of a rotating vat carousel system (including 4 different tanks – Fig. 6a) with a resolution of 20 μm on the z-axis. The same group later introduced more details on the construction and programming steps during operation [47]. Using commercial resins, several multi-material complex ''chess rook'' parts were produced via SLA (Fig. 6b). The development of multi-material micro-SLA was further investigated by Choi *et al.* [48], by creating a system based on a syringe pump that controlled the dispensing of the material into a single build vat. Multi-material items were successfully produced using three different resin systems (Fig. 6c and 6d). Although the process included manual intervention for changing the materials and rinsing the parts, the combination of different materials was efficiently demonstrated both within and across layers. More recently, Khatri *et al.* [49] reported the development of a versatile multi-material DLP system allowing printing of UV-curable resins from three different vats. In this study, one vat was filled with isopropanol solvent to ensure computer-controlled rinsing of the printed item before switching between materials.

These pioneering results on multi-material VPP had been achieved by employing classical resins formulation (only polymer matrix and photoinitiator). No doubt that future years will witness the emergence of multi-material VPP of composite materials. Such a milestone would definitely revolutionize the additive manufacturing field and pave the way towards printability of complete functional devices for diverse applications including complete energy storage devices and other electronics. Electrochemical characterization of a complete battery that would be obtained through a VPP multi-material option is certainly envisioned.

B. SINTERED ITEMS

While the introduction of additional thermal post-processing steps is challenging, the main motivation for sintering printed

battery components is the improved electrochemical properties in comparison with the green state counterparts. In this case the polymer matrix is removed, leaving the resulting item free of ''dead material''. As a consequence, a high degree of porosity is left and the item is constituted mainly from electroactive material. This porosity can be filled with a liquid electrolyte, which would result in an accessible route for the lithium ions. Upon cycling, sintered electrodes will exhibit greater specific capacity, capacity retention over time, energy and power density, in comparison with green state items. Since battery performances are also associated with the electronic conductivity, the presence of pure poorly conductive electroactive materials such as $LiFePO_4$, $LiCoO_2$ or $Li_4Ti_5O_{12}$ must be coupled with the introduction of conductive carbonaceous materials. The sintering of 3D printed ceramic electrolytes and current collectors is expected to considerably increase the ionic and electronic conductivities, respectively, but at the expense of the mechanical performance. The shrinkage occurring during the sintering of a printed item with a simple geometry can be estimated with a scaling law, but is difficult to predict for non-uniform geometries where anisotropic shrinkage can occur. In this context, the resulting shape-conformable battery, originally designed to fit perfectly in the available space, might be compromised. Other issues such as delamination between layers and eventual collapse of the printed piece can be avoided by thoroughly investigating temperature rates and dwell times during both debinding and sintering steps, for example with the use of thermogravimetric analysis. The debinding is a delicate process, the item can crack, blister, or damage, leading most of the times to structural collapse when following an improperly designed thermal cycle. To circumvent these issues, long heating cycles with controlled heating ramps are often used.

Prior to performing any electrochemical characterization, the production of a complete battery in one single print (green part) using a multi-material VPP process could also be subjected to thermal treatment to enhance the resulting performance. An important stage resides in the ability of the printed multi-material structure to maintain structural integrity from the mechanical standpoint. Here, the debinding and sintering temperatures must be tuned depending on the polymeric matrix and/or electroactive materials. Indeed, performing the thermal treatment of a printed battery composed of several different components (electrodes, electrolyte, current collectors) in a single cycle is clearly a challenging task that is yet to be overcome.

IV. VPP OF BATTERIES VIA ALTERNATIVE APPROACHES

While 3D printing LIB components from resins loaded with solid electroactive particles has not yet been demonstrated, the initial studies of 3D printed LIB components via laser and projection VPP started to emerge from 2017 using alternative approaches: **1)** 3D printing of a pure polymer scaffold structure followed by the deposition or introduction of the electroactive materials, **2)** soluble components added to the resin (no thermal treatment needed) for separator, gel or solid polymer electrolyte printing, and **3)** battery precursors added to the resin and electroactive materials synthesized in situ during the sintering step. A summary is displayed in Table 2.

A. SCAFFOLD APPROACH

The initial approach for printing complex structures to be employed as scaffolds for battery components was reported by Cohen *et al.* [50]. The authors employed thermoplastic material extrusion and vat photopolymerization to produce complex 3D lattice structures from commercial thermoplastic filaments and UV-curable resins, respectively. On top of conductive scaffolds (polylactic acid-graphene 92:8 wt.%) printed via thermoplastic material extrusion, tri-layered arrangements of $LiFePO_4$ as cathode, $LiAlO_2$-Polyethylene oxide or $Li_{1+x}Al_yGe_{2-y}(PO_4)_3$-Polyethylenimine membrane as separator, and $Li_4Ti_5O_{12}$ as anode, were built by electrophoretic deposition. The resulting micro-battery was reported to offer high reversible specific capacity and high pulse-power capability compared to commercial planar thin-film batteries. As suggested by the authors, similar work could be performed with higher resolution VPP processes.

Similarly, Zekoll *et al.* [51] prepared a hybrid electrolyte composed of 3D micro-channels of $Li_{1.4}Al_{0.4}Ge_{1.6}(PO_4)_3$ ceramic solid electrolyte and non-conducting polymers (epoxy polymer and polypropylene). The porous polymer framework was primarily achieved via 2PP (Fig. 7a) whereas the remaining empty space was filled with the $Li_{1.4}Al_{0.4}Ge_{1.6}(PO_4)_3$ ceramic powder. Finally, the structure was placed in a furnace to eliminate the polymer matrix and perform sintering of the $Li_{1.4}Al_{0.4}Ge_{1.6}(PO_4)_3$ 3D arrangement. Cubic, diamond-shaped and gyroidal microarchitectures were produced. Higher performances were found with the gyroid $Li_{1.4}Al_{0.4}Ge_{1.6}(PO_4)_3$ structure proving an ionic conductivity of 1.6×10^{-4} S/cm at ambient temperature.

B. SOLUBLE COMPONENTS APPROACH FOR SEPARATOR, GEL, OR SOLID POLYMER ELECTROLYTE

The synthesis of resins to serve as separator, gel polymer electrolyte, ionogel, solid polymer electrolyte after printing has also been investigated [52]–[55]. This trend can be simply justified by the easier resin formulation of these components as the incorporation of solid particles is not required (in comparison to the resin formulation for electrodes or ceramic electrolytes, where solid fillers are often incorporated). Good printability of the resin is therefore facilitated as no particle sedimentation occurs. Furthermore, the viscosity of the resin can be tuned and delamination between printed layers is not prone to occur. Moreover, it is worth emphasizing that the resulting separator, gel or solid polymer electrolyte green parts (obtained just after printing) do not require any additional thermal post-process before undergoing traditional battery assembly and cycling.

TABLE 2. Composite resin formulation, 3D-priniting process and resulting electrochemical properties of the printed battery components from studies reported in literature.

Approach	Battery component (chemistry)	Photocurable resin composition	3D-printing process and parameters	Post-treatment (if any) and resulting electrochemical performances	Reference
Scaffold	Solid ceramic electrolyte (Li-ion)	Commercial resin	2PP Layer thickness: 1 µm	Filling of the printed lattice structure with $Li_{1.4}Al_{0.4}Ge_{1.6}(PO_4)_3$ powder followed by sintering at 900 ºC; Ionic conductivity: 1.6×10^{-4} S/cm at ambient temperature	[51]
Soluble components	Gel polymer electrolyte (Li-ion)	Monomer: PEGDA (Mn=575) Photoabsorber: Sudan I Photoinitiator: TPO Liquid electrolyte: 1M $LiClO_4$ in ethylene carbonate / propylene carbonate	µSLA Layer thickness: 10 µm	GPE ionic conductivity: 4.8×10^{-3} S/cm at room temperature; Capacity: 1.4 µAh/cm^2 at 2 µA during 5 cycles in a $LiFePO_4$|3D printed GPE|$Li_4Ti_5O_{12}$ configuration	[52]
		Monomers: N,N-dimethyl acrylamide; poly(vinylidene fluoride) Crosslinker: divinyl benzene Photoabsorber: Kemisorp 11S Photoinitiator: α-ketoglutonic acid Liquid electrolyte: LiCl in ethylene glycol	SLA	GPE ionic conductivity: 6.5×10^{-4} S/cm at room temperature	[53]
	Ionogel (Li-ion)	Commercial resin Ionic liquids: 1-methyl-3-(4-sulfobutyl)imidazolium para-toluenesulfonate; 1-methyl-1-butylpiperidiniumsulfonate para-toluenesulfonate;1-methyl-3-(4-sulfobutyl) imidazolium methylsulfonate)	SLA	Ionogel ionic conductivity: up to 0.7×10^{-4} S/cm at room temperature and 3.4×10^{-3} S/cm at 90 ºC	[55]
	Solid polymer electrolyte (Li-ion)	Monomer: PEGDA (Mv=1000) Photoinitiator: TPO Lithium salt: lithium bis(trifluoromethanesulfonyl)imide	SLA	SPE ionic conductivity: 3.7×10^{-4} S/cm at 25 ºC; Capacity: 166 mAh/g at 0.1C at 50 ºC and 77% capacity retention after 250 cycles in a $LiFePO_4$|3D printed SPE|Li metal configuration	[54]
Precursor	Positive electrode (Li-ion)	Monomer: PEGDA (Mn=575) Photoabsorber: Tartrazine Photoinitiator: lithium phenyl-2,4,6-trimethylbenzoylphosphinate Metal precursors: lithium nitrate; cobalt nitrate hexahydrate	DLP Layer thickness: 150 µm	$LiCoO_2$ electroactive material is synthesized upon sintering at 700 ºC; Capacity: 121 mAh/g at C/40 and 76% capacity retention after 100 cycles when tested vs Li metal	[65]
	Positive electrode (Li-S)	Commercial resin Surfactants: polyvinylpyrrolidone; polysorbate-20 Metal precursor: $Li_2SO_4.H_2O$	DLP Layer thickness: 50 µm	Li_2S-C electroactive material is synthesized upon sintering at 800 ºC; First cycle capacity: 310 mAh/g of active material at C/20 and 80% capacity retention after 100 cycles when tested vs Li metal	[66]

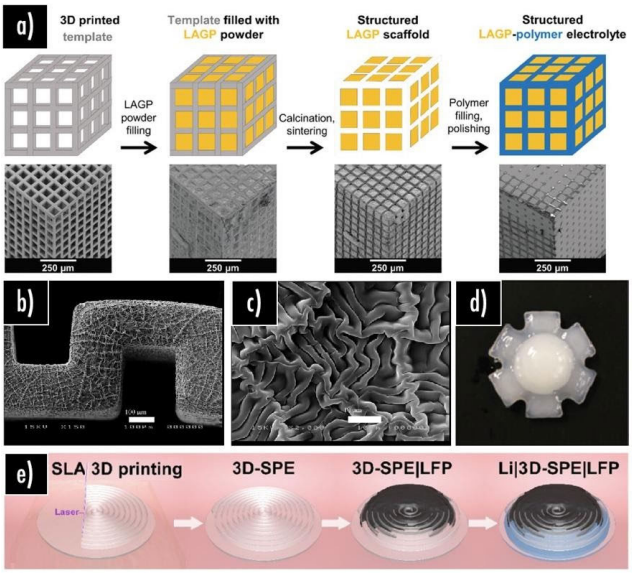

FIGURE 7. **(a) Template procedure used for the synthesis of structured hybrid electrolytes [51], (b) and (c) SEM images of a 3D printed zigzag gel polymer electrolyte structure [52], (d) images of 3D printed flower shape gel electrolyte [53], and (e) preparation process of an all-solid-state lithium metal batteries using an SLA 3D printed solid polymer electrolyte spiral membrane [54].**

For the first time in 2017, Chen *et al.* [52] reported the elaboration of a gel polymer electrolyte by printing a mixture (20/80 in vol%) of UV-curable resin with a 1M $LiClO_4$ in an ethylene carbonate/propylene carbonate (v/v 1/1) liquid electrolyte using the μSLA process. The authors were able to print a zig-zag membrane (Fig. 7b and 7c) exhibiting an ionic conductivity of 4.8×10^{-3} S/cm at room temperature. Then, the complete battery was assembled by filling both sides with electrode slurries (gel polymer electrolyte-$LiFePO_4$ and gel polymer electrolyte-$Li_4Ti_5O_{12}$) and adding an aluminum foil as a current collector. The resulting micro-battery was galvanostatically tested and exhibited a capacity of 1.4 $\mu Ah/cm^2$ at a discharging current of 2 μA for two cycles according to the authors.

Additional work was reported by Rahman *et al.* [53] to tune the mechanical properties and favor the thermal stability of the resulting printed gel polymer electrolyte membrane. They reported the preparation and printability of a UV-curable poly(vinylidene fluoride) (PVDF)/N,N-dimethyl acrylamide (DMAA)-based resin comprising LiCl as a lithium salt and ethylene glycol (EG) as solvent (Fig. 7d). An ionic conductivity as high as 6.5×10^{-4} S/cm was achieved at room temperature for the optimized membrane composition (PVDF/DMAA/LiCl/EG wt.% 5/45/5/45).

Based on a similar approach, Zehbe *et al.* [55] demonstrated that laser VPP can produce complex ionogels structures. In this study, the authors prepared resins composed of sulfonate-based ionic liquids (80 wt.%) (1-methyl-3-(4-sulfobutyl)imidazolium para-toluenesulfonate, 1-methyl-1-butylpiperidiniumsulfonate para-toluenesulfonate and 1-methyl-3-(4-sulfobutyl) imidazolium methylsulfonate) mixed with a commercial UV-curable resin (20 wt.%). Upon printing, the ionogels exhibited ionic conductivities up to 0.7×10^{-4} S/cm and 3.4×10^{-3} S/cm at room temperature and at 90 °C, respectively. The resulting membranes were shown to be mechanically robust and thermally stable up to 200 °C.

Focused on the development of a solid polymer electrolyte via VPP, He *et al.* [54] prepared a PEGDA-based resin containing phenylbis(2,4,6-trimethylbenzoyl)-phosphine oxide as photoinitiator and lithium bis(trifluoromethanesulfonyl) imide (LiTFSI) as lithium salt. A 3D-printed archimedean spiral-shaped solid polymer electrolyte (Fig. 7e) exhibiting an ionic conductivity of 3.7×10^{-4} S/cm at 25 °C was obtained, and was later galvanostatically tested in an all-solid-state lithium metal battery configuration (Li|3D-solid polymer electrolyte |$LiFePO_4$). A capacity value of 166 mAh/g at a current density of 0.1C at 50°C and a capacity retention of 77% after 250 cycles was reported. The spiral-shaped solid polymer electrolyte was shown to greatly reinforce interfacial adhesion. A similar VPP approach could be undoubtedly transposed to other methacrylate-based solid polymer electrolytes, such as the methyl acrylate functionalized poly(D,L-Lactide)/poly(ethylene glycol) methyl ether methacrylate with LiTFSI as lithium salt and Irgacure 1173 as photoinitiator, proposed by Zaheer *et al.* [56]. In this study, the authors obtained a 2D film after the UV illumination step, but 3D complex geometries could theoretically be produced via VPP.

C. PRECURSOR APPROACH: IN SITU SYNTHESIS OF THE ELECTROACTIVE MATERIAL UPON THERMAL TREATMENT

With a view to circumvent the increased resin viscosity associated with the introduction of solid particles, alternatively, 3D printing of electrodes can be achieved by introducing soluble electroactive precursors into the resin and obtaining the electroactive material upon the sintering step. The clear advantage of this approach is that the precursor salts are mixed at the molecular level thanks to their solubility in the resin, and therefore do not promote UV light-scattering during 3D printing. The photopolymerization process is therefore more efficient and accurate compared to the photocuring of conventional powder-loaded resins. After printing, the green part must endure the thermal post-processing steps where the in situ synthesis of the electroactive material or ceramic particles occurs, to form the final self-standing item.

This approach has been optimized over the years to obtain ceramics for all kinds of applications [57]. An example is the use of preceramic polymers such as polysiloxanes or polycarboxiloxanes, that upon thermal treatment above or at 1100°C produces SiC, SiCN, or SiOC ceramics [58-60]. Similarly, Moore *et al.* [61] recently demonstrated the in situ synthesis of 3D structures based on boro-phosphosilicate glasses (SiO_2–B_2O_3–P_2O_5) from a resin composed of poly(diethoxysiloxane), triethyl phosphate and trimethyl borate as soluble precursors for silicon, phosphorus and boron oxides, respectively (Fig. 8). Another example is the synthesis

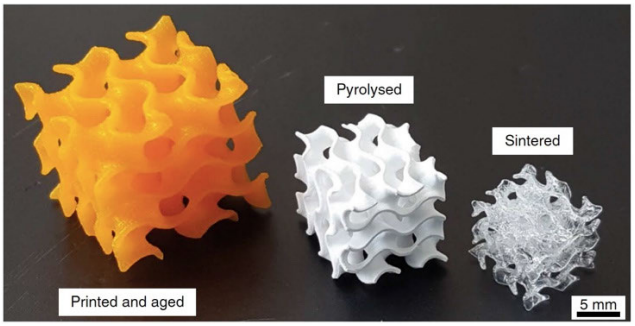

FIGURE 8. Different stages of the production of a SiO_2–B_2O_3–P_2O_5 gyroid glass printed via DLP [61].

of ultralight and ultra-strong ZrOC structures upon thermal treatment at 1200 °C of a DLP-printed structure (Fig. 9a). The resin consisted of a mixture of zirconium n-propoxide and an acrylate-based resin [62]. These examples, among others [63], [64], are a testament of the potential of electroactive oxides to be obtained following this approach.

Frequently encountered problems after sintering classical ceramic materials are non-homogeneous shrinkage, heavy mass loss, poor densification, cracking, weak mechanical performance, and undesirable surface roughness [57]. For battery materials, challenges are expected in every step of the manufacturing process. Among the expected challenges are: determining suitable precursor compounds and stoichiometries, obtaining rheological properties of the precursor resin that allow 3D printing of self-standing structures, and finding appropriate thermal post-processing conditions for the synthesis of battery materials and the elimination of non-electroactive components.

Specifically focused on LIB, Yee *et al.* [65] reported the synthesis of $LiCoO_2$ via projection VPP. In this case, an aqueous PEGDA-based resin was loaded with $Co(NO_3)_2.6H_2O$ and $LiNO_3$ in stoichiometric ratios, from which a hydrogel was printed and calcinated at 700 °C (Fig. 9b and 9c). SEM-energy dispersive X-ray analysis demonstrated that 7.5 atomic% of foreign elements (C, Na, P, Al, S and Si) were left after the calcination process, but the authors stated that this amount can be reduced by better controlling the thermal post-processing conditions. From this 3D structure an initial capacity of 121 mAh/g (theoretical capacity of 140 mAh/g) at C/40 in half-cell versus lithium was obtained. The capacity retention over 100 cycles at C/10 was shown to be 76%. Capacity loss can be explained by the large ohmic impedance due to the electrode thickness, lack of conductive additives, and progressive structural collapse upon cycling.

In regular ceramics, any kind of porosity must be avoided because its presence can lead to cracking during thermal post-processing. In contrast, 3D printed electrodes require a certain micro-porosity, so that adequate electrolyte impregnation is allowed. To address this issue, Yee *et al.* [65] worked on the tuning ratio of PEGDA-to-$LiCoO_2$, and found that by increasing the lithium precursor, it was possible to increase the micro-porosity without excessively increasing the Ohmic impedance. Two other methods to promote micro-porosity

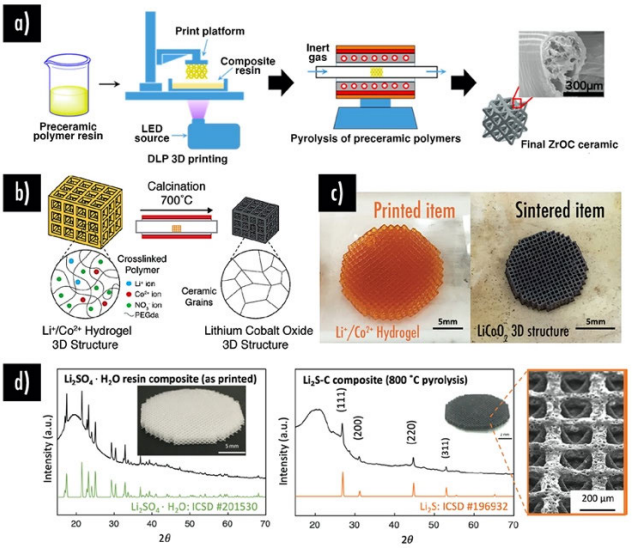

FIGURE 9. (a) Precursor approach preparation scheme [62]; (b) Schematic of the sintering of the 3D Li^+/Co^{2+} hydrogel to obtain the 3D LCO structure [65]; (c) Optical images of the 3D Li^+/Co^{2+} hydrogel and LCO structures [65]; (d) XRD patterns and optical images (inset) of the green and brown parts to demonstrate phase change after pyrolysis [66].

are also mentioned. The first is to increase the surface area-to-volume ratio, in order to evacuate in a controlled manner the thermal decomposition gases. The second is to reduce the formation rate of decomposition gases through a combined temperature and vacuum protocol.

On a similar note, Saccone *et al.* [66] recently published the production of a robust and expansion-tolerant Li_2S-C positive electrode for Li-sulfur batteries. Li_2S-C was obtained from the pyrolysis at 800 °C of 3D printed electrodes via projection VPP (Fig. 9d) from an acrylate-based UV-curable resin containing $Li_2SO_4.H_2O$ and surfactants. Surprisingly, the structure presented promising first discharge capacity of 310 mAh/g at C/20 and a retention of 80% after 100 cycles when tested in half-cell configuration versus lithium. It is worth noting that these pioneering studies [65, 66], cycled independent 3D electrodes against a lithium foil (planar structure), resulting in 2.5D batteries [67], as the lithium-ion diffusion is relegated only to two dimensions. In all, these promising efforts demonstrated that VPP of precursor UV-curable resins for battery applications is achievable and highlighted the potential to manufacture 3D designs that were previously thought impossible.

Another important feature to consider when designing battery architectures is the layer resolution. Conventional VPP machines can go as low as few micrometers with optimized printing parameters (exposure time and brightness). Alternatively, 2PP, the highest-resolution additive manufacturing technology currently, could be used to reach details in the nanoscale. At the present time, there are no examples of battery 3D printing via 2PP. However, 2PP printing of preceramic resins followed by in situ synthesis has been reported for other applications [68]–[72]. Brigo *et al.* [68] obtained

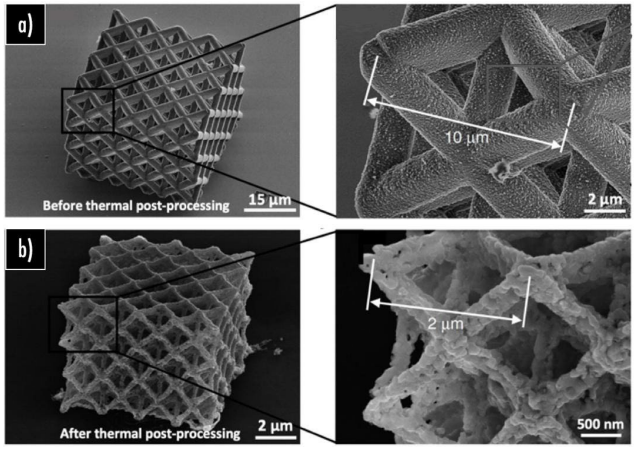

FIGURE 10. (a) Two magnifications of an octet lattice structure printed via 2PP using a resin containing nickel precursors. (b) The same nickel lattice with nanoscale features obtained after sintering [71].

dense SiOC structures with height of 100 μm and 450 nm features after calcination at 1000 °C of the 2PP printed structures. The precursor resin was a commercial acrylate siloxane loaded with bis(dimethylamino)benzophenone as a radical initiator [68]. Similarly, Greer's group printed zinc oxide architectures from a PEGDA-based resin loaded with zinc nitrate hexahydrate [70] and nickel lattices from an acrylic-based resin containing nickel acrylate (Fig. 10) [71]. These works pave the way towards the fabrication of ceramic electrode and electrolyte 3D structures via 2PP.

V. CONCLUSION

3D printing techniques allow the development of energy storage devices such as LIB based on a layer-by-layer material deposition, offering the possibility to manufacture shape-conformable structures with intricate 3D geometries to enhance the power performance, while reducing electrochemically inactive weight and volume. VPP has the potential to revolutionize the fabrication of batteries based on the improved spatial resolution (main advantage) compared to other additive manufacturing subcategories such as material extrusion. Although VPP has not been extensively used to fabricate batteries for now, the demand for shape-conformable and high-power devices makes this topic particularly promising. The work on ceramic resin formulation and printing that has been previously reported for other applications such as dentistry or electronics, can certainly be transposed to batteries. An important research threshold still involves the composite resin development through the introduction of solid electroactive particles or by employing a precursor approach. The impact of the added fillers on the viscosity of the resin and the light path are the main two key-points that must be studied thoroughly. Finally, studying the impact of the printing parameters as well as the development and optimization of multi-material printers will undoubtedly pave the way towards the manufacturing of a complete high-resolution shape conformable 3D battery via VPP.

ACKNOWLEDGMENT

(Alexis Maurel and Ana C. Martinez contributed equally to this work.)

REFERENCES

[1] J. W. Long, B. Dunn, D. R. Rolison, and H. S. White, "Three-dimensional battery architectures," *Chem. Rev.*, vol. 104, no. 10, pp. 4463–4492, Oct. 2004, doi: 10.1021/cr0207401.

[2] A. Maurel, M. Haukka, E. MacDonald, L. Kivijärvi, E. Lahtinen, H. Kim, M. Armand, A. Cayla, A. Jamali, S. Grugeon, L. Dupont, and S. Panier, "Considering lithium-ion battery 3D-printing via thermoplastic material extrusion and polymer powder bed fusion," *Additive Manuf.*, vol. 37, Jan. 2021, Art. no. 101651, doi: 10.1016/j.addma.2020.101651.

[3] B. Trembacki, E. Duoss, G. Oxberry, M. Stadermann, and J. Murthy, "Mesoscale electrochemical performance simulation of 3D interpenetrating lithium-ion battery electrodes," *J. Electrochem. Soc.*, vol. 166, no. 6, pp. A923–A934, Mar. 2019, doi: 10.1149/2.0031906jes.

[4] H.-S. Min, B. Y. Park, L. Taherabadi, C. Wang, Y. Yeh, R. Zaouk, M. J. Madou, and B. Dunn, "Fabrication and properties of a carbon/polypyrrole three-dimensional microbattery," *J. Power Sources*, vol. 178, no. 2, pp. 795–800, Apr. 2008, doi: 10.1016/j.jpowsour.2007.10.003.

[5] G. Oltean, L. Nyholm, and K. Edström, "Galvanostatic electrodeposition of aluminium nano-rods for Li-ion three-dimensional micro-battery current collectors," *Electrochim. Acta*, vol. 56, no. 9, pp. 3203–3208, Mar. 2011, doi: 10.1016/j.electacta.2011.01.053.

[6] M. Roberts, P. Johns, J. Owen, D. Brandell, K. Edstrom, G. E. Enany, C. Guery, D. Golodnitsky, M. Lacey, C. Lecoeur, H. Mazor, E. Peled, E. Perre, M. M. Shaijumon, P. Simonc, and P.-L. Tabernac, "3D lithium ion batteries—From fundamentals to fabrication," *J. Mater. Chem.*, vol. 21, no. 27, pp. 9876–9890, 2011, doi: 10.1039/c0jm04396f.

[7] A. Maurel, "Thermoplastic composite filaments formulation and 3D-printing of a lithium-ion battery via fused deposition modeling," Ph.D. dissertation, Dept. Chem., Univ. Picardie Jules Verne, Amiens, France, 2020.

[8] H. Ragones, S. Menkin, Y. Kamir, A. Gladkikh, T. Mukra, G. Kosa, and D. Golodnitsky, "Towards smart free form-factor 3D printable batteries," *Sustain. Energy Fuels*, vol. 2, no. 7, pp. 1542–1549, 2018, doi: 10.1039/c8se00122g.

[9] L. E. Asp, K. Bouton, D. Carlstedt, S. Duan, R. Harnden, W. Johannisson, M. Johansen, M. K. G. Johansson, G. Lindbergh, F. Liu, K. Peuvot, L. M. Schneider, J. Xu, and D. Zenkert, "A structural battery and its multifunctional performance," *Adv. Energy Sustain. Res.*, vol. 2, no. 3, Mar. 2021, Art. no. 2000093, doi: 10.1002/aesr.202000093.

[10] A. Maurel, S. Grugeon, M. Armand, B. Fleutot, M. Courty, K. Prashantha, C. Davoisne, H. Tortajada, S. Panier, and L. Dupont, "Overview on lithium-ion battery 3D-printing by means of material extrusion," *ECS Trans.*, vol. 98, no. 13, pp. 3–21, Sep. 2020, doi: 10.1149/09813.0003ecst.

[11] S.-H. Kim, K.-H. Choi, S.-J. Cho, S. Choi, S. Park, and S.-Y. Lee, "Printable solid-state lithium-ion batteries: A new route toward shape-conformable power sources with aesthetic versatility for flexible electronics," *Nano Lett.*, vol. 15, no. 8, pp. 5168–5177, Aug. 2015, doi: 10.1021/acs.nanolett.5b01394.

[12] K. Sun, T. Wei, B. Y. Ahn, J. Y. Seo, S. J. Dillon, and J. A. Lewis, "3D printing of interdigitated Li-ion microbattery architectures," *Adv. Mater.*, vol. 25, no. 33, pp. 4539–4543, Sep. 2013, doi: 10.1002/adma.201301036.

[13] T. Wei, B. Y. Ahn, J. Grotto, and J. A. Lewis, "3D printing of customized Li-ion batteries with thick electrodes," *Adv. Mater.*, vol. 30, no. 16, Apr. 2018, Art. no. 1703027, doi: 10.1002/adma.201703027.

[14] K. Fu, Y. Wang, C. Yan, Y. Yao, Y. Chen, J. Dai, S. Lacey, Y. Wang, J. Wan, T. Li, Z. Wang, Y. Xu, and L. Hu, "Graphene oxide-based electrode inks for 3D-printed lithium-ion batteries," *Adv. Mater.*, vol. 28, no. 13, pp. 2587–2594, Apr. 2016, doi: 10.1002/adma.201505391.

[15] J. Li, X. Liang, F. Liou, and J. Park, "Macro-/micro-controlled 3D lithium-ion batteries via additive manufacturing and electric field processing," *Sci. Rep.*, vol. 8, no. 1, Jan. 2018, Art. no. 1846, doi: 10.1038/s41598-018-20329-w.

[16] A. Maurel, M. Courty, B. Fleutot, H. Tortajada, K. Prashantha, M. Armand, S. Grugeon, S. Panier, and L. Dupont, "Highly loaded graphite–polylactic acid composite-based filaments for lithium-ion battery three-dimensional printing," *Chem. Mater.*, vol. 30, no. 21, pp. 7484–7493, Nov. 2018, doi: 10.1021/acs.chemmater.8b02062.

[17] A. Maurel, S. Grugeon, B. Fleutot, M. Courty, K. Prashantha, H. Tortajada, M. Armand, S. Panier, and L. Dupont, "Three-dimensional printing of a $LiFePO_4$/graphite battery cell via fused deposition modeling," *Sci. Rep.*, vol. 9, no. 1, p. 18031, Dec. 2019, doi: 10.1038/s41598-019-54518-y.

[18] C. Reyes, R. Somogyi, S. Niu, M. A. Cruz, F. Yang, M. J. Catenacci, C. P. Rhodes, and B. J. Wiley, "Three-dimensional printing of a complete lithium ion battery with fused filament fabrication," *ACS Appl. Energy Mater.*, vol. 1, no. 10, pp. 5268–5279, Oct. 2018, doi: 10.1021/acsaem.8b00885.

[19] H. Ragones, A. Vinegrad, G. Ardel, M. Goor, Y. Kamir, M. M. Dorfman, A. Gladkikh, and D. Golodnitsky, "On the road to a multi-coaxial-cable battery: Development of a novel 3D-printed composite solid electrolyte," *J. Electrochem. Soc.*, vol. 167, no. 7, Dec. 2019, Art. no. 070503, doi: 10.1149/2.0032007jes.

[20] A. Z. Zhakeyev and L. Xuan, "Photoactive resin formulations and composites for optical 3D and 4D printing of functional materials and devices," in *3D and 4D Printing of Polymer Nanocomposite Materials: Processes, Applications, and Challenges*, 1st ed. Amsterdam, The Netherlands: Elsevier, 2019, ch. 13, p. 592.

[21] H. Bikas, P. Stavropoulos, and G. Chryssolouris, "Additive manufacturing methods and modelling approaches: A critical review," *Int. J. Adv. Manuf. Technol.*, vol. 83, nos. 1–4, pp. 389–405, Mar. 2016, doi: 10.1007/s00170-015-7576-2.

[22] W. Yang, H. Yu, W. Liang, Y. Wang, and L. Liu, "Rapid fabrication of hydrogel microstructures using UV-induced projection printing," *Micromachines*, vol. 6, no. 12, pp. 1903–1913, Dec. 2015, doi: 10.3390/mi6121464.

[23] A. Bagheri and J. Jin, "Photopolymerization in 3D printing," *ACS Appl. Polym. Mater.*, vol. 1, no. 4, pp. 593–611, Apr. 2019, doi: 10.1021/acsapm.8b00165.

[24] L. J. Y. Tan, W. Zhu, and K. Zhou, "Recent progress on polymer materials for additive manufacturing," *Adv. Funct. Mater.*, vol. 30, no. 43, Oct. 2020, Art. no. 2003062, doi: 10.1002/adfm.202003062.

[25] S. J. Leigh, C. P. Purssell, J. Bowen, D. A. Hutchins, J. A. Covington, and D. R. Billson, "A miniature flow sensor fabricated by micro-stereolithography employing a magnetite/acrylic nanocomposite resin," *Sens. Actuators A, Phys.*, vol. 168, no. 1, pp. 66–71, Jul. 2011, doi: 10.1016/j.sna.2011.03.058.

[26] B. Steyrer, B. Busetti, G. Harakály, R. Liska, and J. Stampfl, "Hot lithography vs. room temperature DLP 3D-printing of a dimethacrylate," *Additive Manuf.*, vol. 21, pp. 209–214, May 2018, doi: 10.1016/j.addma.2018.03.013.

[27] D. Yugang, Z. Yuan, T. Yiping, and L. Dichen, "Nano-TiO_2-modified photosensitive resin for RP," *Rapid Prototyping J.*, vol. 17, no. 4, pp. 247–252, Jun. 2011, doi: 10.1108/13552541111138360.

[28] C. Hinczewski, S. Corbel, and T. Chartier, "Ceramic suspensions suitable for stereolithography," *J. Eur. Ceram. Soc.*, vol. 18, no. 6, pp. 583–590, 1998, doi: 10.1016/s0955-2219(97)00186-6.

[29] M. Schwentenwein and J. Homa, "Additive manufacturing of dense alumina ceramics," *Int. J. Appl. Ceram. Technol.*, vol. 12, no. 1, pp. 1–7, Jan. 2015, doi: 10.1111/ijac.12319.

[30] K. F. Brakora and K. Sarabandi, "Integration of single-mode photonic crystal clad waveguides with monolithically constructed ceramic subsystems," *IEEE Antennas Wireless Propag. Lett.*, vol. 8, pp. 433–436, 2008, doi: 10.1109/lawp.2008.2007991.

[31] M. L. Griffith and J. W. Halloran, "Freeform fabrication of ceramics via stereolithography," *J. Amer. Ceram. Soc.*, vol. 79, no. 10, pp. 2601–2608, Aug. 2005.

[32] H. Liu and J. Mo, "Study on nanosilica reinforced stereolithography resin," *J. Reinforced Plastics Compos.*, vol. 29, no. 6, pp. 909–920, Mar. 2010, doi: 10.1177/0731684409102838.

[33] W. Dong, H. Ma, R. Liu, T. Liu, S. Li, C. Bao, and S. Song, "Fabrication by stereolithography of fiber-reinforced fused silica composites with reduced crack and improved mechanical properties," *Ceram. Int.*, vol. 47, no. 17, pp. 24121–24129, Sep. 2021, doi: 10.1016/j.ceramint.2021.05.123.

[34] Z. Tian, Y. Yang, Y. Wang, H. Wu, W. Liu, and S. Wu, "Fabrication and properties of a high porosity h-BN–SiO_2 ceramics fabricated by stereolithography-based 3D printing," *Mater. Lett.*, vol. 236, pp. 144–147, Feb. 2019, doi: 10.1016/j.matlet.2018.10.058.

[35] K. Zhang, R. He, C. Xie, G. Wang, G. Ding, M. Wang, W. Song, and D. Fang, "Photosensitive ZrO_2 suspensions for stereolithography," *Ceram. Int.*, vol. 45, no. 9, pp. 12189–12195, Jun. 2019, doi: 10.1016/j.ceramint.2019.03.123.

[36] N. Travitzky, A. Bonet, B. Dermeik, T. Fey, I. Filbert-Demut, L. Schlier, T. Schlordt, and P. Greil, "Additive manufacturing of ceramic-based materials," *Adv. Eng. Mater.*, vol. 16, no. 6, pp. 729–754, Jun. 2014, doi: 10.1002/adem.201400097.

[37] G. Mitteramskogler, R. Gmeiner, R. Felzmann, S. Gruber, C. Hofstetter, J. Stampfl, J. Ebert, W. Wachter, and J. Laubersheimer, "Light curing strategies for lithography-based additive manufacturing of customized ceramics," *Additive Manuf.*, vols. 1–4, pp. 110–118, Oct. 2014, doi: 10.1016/j.addma.2014.08.003.

[38] S. P. Gentry and J. W. Halloran, "Light scattering in absorbing ceramic suspensions: Effect on the width and depth of photopolymerized features," *J. Eur. Ceram. Soc.*, vol. 35, no. 6, pp. 1895–1904, Jun. 2015, doi: 10.1016/j.jeurceramsoc.2014.12.006.

[39] S. H. Park, M. Kaur, D. Yun, and W. S. Kim, "Hierarchically designed electron paths in 3D printed energy storage devices," *Langmuir*, vol. 34, no. 37, pp. 10897–10904, Sep. 2018, doi: 10.1021/acs.langmuir.8b02404.

[40] Y. Yang, Z. Chen, X. Song, B. Zhu, T. Hsiai, P.-I. Wu, R. Xiong, J. Shi, Y. Chen, Q. Zhou, and K. K. Shung, "Three dimensional printing of high dielectric capacitor using projection based stereolithography method," *Nano Energy*, vol. 22, pp. 414–421, Apr. 2016, doi: 10.1016/j.nanoen.2016.02.045.

[41] A. Maurel, R. Russo, S. Grugeon, S. Panier, and L. Dupont, "Environmentally friendly lithium-terephthalate/polylactic acid composite filament formulation for lithium-ion battery 3D-printing via fused deposition modeling," *ECS J. Solid State Sci. Technol.*, vol. 10, no. 3, Mar. 2021, Art. no. 037004, doi: 10.1149/2162-8777/abedd4.

[42] G. L. Goh, H. Zhang, T. H. Chong, and W. Y. Yeong, "3D printing of multilayered and multimaterial electronics: A review," *Adv. Electron. Mater.*, vol. 7, no. 10, Oct. 2021, Art. no. 2100445, doi: 10.1002/aelm.202100445.

[43] B. H. Lu, H. B. Lan, and H. Z. Liu, "Additive manufacturing frontier: 3D printing electronics," *Opto-Electron. Adv.*, vol. 1, no. 1, 2018, Art. no. 17000401, doi: 10.29026/oea.2018.170004.

[44] R. Hensleigh, H. Cui, Z. Xu, J. Massman, D. Yao, J. Berrigan, and X. Zheng, "Charge-programmed three-dimensional printing for multi-material electronic devices," *Nature Electron.*, vol. 3, no. 4, pp. 216–224, Apr. 2020, doi: 10.1038/s41928-020-0391-2.

[45] D. Qiu and N. A. Langrana, "Void eliminating toolpath for extrusion-based multi-material layered manufacturing," *Rapid Prototyping J.*, vol. 8, no. 1, pp. 38–45, Mar. 2002, doi: 10.1108/13552540210413293.

[46] A. Inamdar, M. Magana, F. Medina, Y. Grajeda, and R. B. Wicker, "Development of an automated multiple material stereolithography machine," in *Proc. SFF Symp.*, Austin, TX, USA, 2006, pp. 624–635.

[47] J.-W. Choi, H.-C. Kim, and R. Wicker, "Multi-material stereolithography," *J. Mater. Process. Technol.*, vol. 211, no. 3, pp. 318–328, Mar. 2011, doi: 10.1016/j.jmatprotec.2010.10.003.

[48] J.-W. Choi, E. MacDonald, and R. Wicker, "Multi-material microstereolithography," *Int. J. Adv. Manuf. Technol.*, vol. 49, nos. 5–8, pp. 543–551, Jul. 2010, doi: 10.1007/s00170-009-2434-8.

[49] B. Khatri, M. Frey, A. Raouf-Fahmy, M.-V. Scharla, and T. Hanemann, "Development of a multi-material stereolithography 3D printing device," *Micromachines*, vol. 11, no. 5, p. 532, May 2020, doi: 10.3390/mi11050532.

[50] E. Cohen, S. Menkin, M. Lifshits, Y. Kamir, A. Gladkich, G. Kosa, and D. Golodnitsky, "Novel rechargeable 3D-microbatteries on 3D-printed-polymer substrates: Feasibility study," *Electrochim. Acta*, vol. 265, pp. 690–701, Mar. 2018, doi: 10.1016/j.electacta.2018.01.197.

[51] S. Zekoll, C. Marriner-Edwards, A. K. O. Hekselman, J. Kasemchainan, C. Kuss, D. E. J. Armstrong, D. Cai, R. J. Wallace, F. H. Richter, J. H. J. Thijssen, and P. G. Bruce, "Hybrid electrolytes with 3D bicontinuous ordered ceramic and polymer microchannels for all-solid-state batteries," *Energy Environ. Sci.*, vol. 11, no. 1, pp. 185–201, Jan. 2018, doi: 10.1039/c7ee02723k.

[52] Q. Chen, R. Xu, Z. He, K. Zhao, and L. Pan, "Printing 3D gel polymer electrolyte in lithium-ion microbattery using stereolithography," *J. Electrochem. Soc.*, vol. 164, no. 9, pp. A1852–A1857, 2017, doi: 10.1149/2.0651709jes.

[53] M. S. Rahman, M. N. I. Shiblee, K. Ahmed, A. Khosla, J. Ogawa, M. Kawakami, and H. Furukawa, "Flexible and conductive 3D printable polyvinylidene fluoride and poly(N, N-dimethylacrylamide) based gel polymer electrolytes," *Macromol. Mater. Eng.*, vol. 305, no. 9, Sep. 2020, Art. no. 2000262, doi: 10.1002/mame.202000262.

[54] Y. He, S. Chen, L. Nie, Z. Sun, X. Wu, and W. Liu, "Stereolithography three-dimensional printing solid polymer electrolytes for all-solid-state lithium metal batteries," *Nano Lett.*, vol. 20, no. 10, pp. 7136–7143, Oct. 2020, doi: 10.1021/acs.nanolett.0c02457.

[55] K. Zehbe, A. Lange, and A. Taubert, "Stereolithography provides access to 3D printed ionogels with high ionic conductivity," *Energy Fuels*, vol. 33, no. 12, pp. 12885–12893, Dec. 2019, doi: 10.1021/acs.energyfuels.9b03379.

[56] M. Zaheer, H. Xu, B. Wang, L. Li, and Y. Deng, "An *in situ* polymerized comb-like PLA/PEG-based solid polymer electrolyte for lithium metal batteries," *J. Electrochem. Soc.*, vol. 167, no. 7, Dec. 2019, Art. no. 070504, doi: 10.1149/2.0042007jes.

[57] S. A. Rasaki, D. Xiong, S. Xiong, F. Su, M. Idrees, and Z. Chen, "Photopolymerization-based additive manufacturing of ceramics: A systematic review," *J. Adv. Ceram.*, vol. 10, no. 3, pp. 442–471, Jun. 2021, doi: 10.1007/s40145-021-0468-z.

[58] P. Colombo, G. Mera, R. Riedel, and G. D. Soraru, "Polymer-derived ceramics: 40 years of research and innovation in advanced ceramics," *J. Amer. Ceram. Soc.*, vol. 93, no. 7, pp. 1805–1837, Jul. 2010, doi: 10.1111/j.1551-2916.2010.03876.x.

[59] X. Wang, F. Schmidt, D. Hanaor, P. H. Kamm, S. Li, and A. Gurlo, "Additive manufacturing of ceramics from preceramic polymers: A versatile stereolithographic approach assisted by thiol-ene click chemistry," *Additive Manuf.*, vol. 27, pp. 80–90, May 2019, doi: 10.1016/j.addma.2019.02.012.

[60] Y. de Hazan and D. Penner, "SiC and SiOC ceramic articles produced by stereolithography of acrylate modified polycarbosilane systems," *J. Eur. Ceram. Soc.*, vol. 37, no. 16, pp. 5205–5212, Dec. 2017, doi: 10.1016/j.jeurceramsoc.2017.03.021.

[61] D. G. Moore, L. Barbera, K. Masania, and A. R. Studart, "Three-dimensional printing of multicomponent glasses using phase-separating resins," *Nature Mater.*, vol. 19, no. 2, pp. 212–217, Feb. 2020, doi: 10.1038/s41563-019-0525-y.

[62] Y. Fu, Z. Chen, G. Xu, Y. Wei, and C. Lao, "Preparation and stereolithography 3D printing of ultralight and ultrastrong ZrOC porous ceramics," *J. Alloys Compounds*, vol. 789, pp. 867–873, Jun. 2019, doi: 10.1016/j.jallcom.2019.03.026.

[63] I. Cooperstein, E. Shukrun, O. Press, A. Kamyshny, and S. Magdassi, "Additive manufacturing of transparent silica glass from solutions," *ACS Appl. Mater. Interfaces*, vol. 10, no. 22, pp. 18879–18885, Jun. 2018, doi: 10.1021/acsami.8b03766.

[64] A. Vyatskikh, A. Kudo, S. Delalande, and J. R. Greer, "Additive manufacturing of polymer-derived Titania for one-step solar water purification," *Mater. Today Commun.*, vol. 15, pp. 288–293, Jun. 2018, doi: 10.1016/j.mtcomm.2018.02.010.

[65] D. W. Yee, M. A. Citrin, Z. W. Taylor, M. A. Saccone, V. L. Tovmasyan, and J. R. Greer, "Hydrogel-based additive manufacturing of lithium cobalt oxide," *Adv. Mater. Technol.*, vol. 6, no. 2, Feb. 2021, Art. no. 2000791, doi: 10.1002/admt.202000791.

[66] M. A. Saccone and J. R. Greer, "Understanding and mitigating mechanical degradation in lithium–sulfur batteries: Additive manufacturing of Li_2S composites and nanomechanical particle compressions," *J. Mater. Res.*, no. 66, pp. 1–11, Apr. 2021, doi: 10.1557/s43578-021-00182-w.

[67] K. McKelvey, A. A. Talin, B. Dunn, and H. S. White, "Microscale 2.5D batteries," *J. Electrochem. Soc.*, vol. 164, no. 12, pp. A2500–A2503, 2017, doi: 10.1149/2.0771712jes.

[68] L. Brigo, J. E. M. Schmidt, A. Gandin, N. Michieli, P. Colombo, and G. Brusatin, "3D nanofabrication of SiOC ceramic structures," *Adv. Sci.*, vol. 5, no. 12, Dec. 2018, Art. no. 1800937, doi: 10.1002/advs.201800937.

[69] S. Passinger, M. S. M. Saifullah, C. Reinhardt, K. R. V. Subramanian, B. N. Chichkov, and M. E. Welland, "Direct 3D patterning of TiO_2 using femtosecond laser pulses," *Adv. Mater.*, vol. 19, no. 9, pp. 1218–1221, May 2007, doi: 10.1002/adma.200602264.

[70] D. W. Yee, M. L. Lifson, B. W. Edwards, and J. R. Greer, "Additive manufacturing of 3D-architected multifunctional metal oxides," *Adv. Mater.*, vol. 31, no. 33, Aug. 2019, Art. no. 1901345, doi: 10.1002/adma.201901345.

[71] A. Vyatskikh, S. Delalande, A. Kudo, X. Zhang, C. M. Portela, and J. R. Greer, "Additive manufacturing of 3D nano-architected metals," *Nature Commun.*, vol. 9, no. 1, Feb. 2018, Art. no. 593, doi: 10.1038/s41467-018-03071-9.

[72] T. A. Pham, D.-P. Kim, T.-W. Lim, S.-H. Park, D.-Y. Yang, and K.-S. Lee, "Three-dimensional SiCN ceramic microstructures via nano-stereolithography of inorganic polymer photoresists," *Adv. Funct. Mater.*, vol. 16, no. 9, pp. 1235–1241, Jun. 2006, doi: 10.1002/adfm.200600009.

ALEXIS MAUREL received the B.S. degree in chemistry from the Université Toulouse III Paul Sabatier, in 2015, the M.S. degree in materials for energy storage and conversion from a joint Erasmus+ Program (Poland, Spain, and France), in 2017, and the Ph.D. degree in chemistry of materials from the University of Picardie Jules Verne, Amiens, France, in 2020, for his work on lithium-ion battery 3D printing via thermoplastic material. He is currently a French Fulbright Visiting Scholar at The University of Texas at El Paso, where he is working as a Postdoctoral Researcher. He is an expert on both energy storage and additive manufacturing and currently focusing his research activities on battery 3D printing via vat photopolymerization. He is a member of the Electrochemical Society.

ANA C. MARTINEZ received the B.S. degree in nanotechnology from the Universidad Autó noma de Querétaro, in 2015, the M.S. degree in materials for energy storage and conversion from a joint Erasmus+ Program (Poland, Spain, and France), in 2017, and the Ph.D. degree in chemistry of materials from a joint collaboration between the car manufacturer Renault SAS and the Université de Picardie Jules Verne, France, in 2021. She is currently a Postdoctoral Researcher at the University of Texas at El Paso, in charge of resins formulation and characterization for the 3D printing of diverse battery chemistries. Her research interests include the synthesis of battery materials, batteries for electric vehicles, and advanced characterization.

SYLVIE GRUGEON received the joint B.S. degree from the University of Paris VII, Paris, France, and the University of Picardie Jules Verne, (UPJV) Amiens, France, and the Ph.D. degree in material sciences from UPJV, in 1997. She is currently a Research Engineer with the Laboratoire de Réactivité et de Chimie des Solides, UPJV. Her research interests is focused on the battery field and particularly include the optimization of energy storage devices, safety, electrolyte additives, gas evolution, and 3D printing of lithium-ion batteries.

STÉPHANE PANIER received the Ph.D. degree from the Universitédes Sciences et Technologies de Lille (Lille I), France. He is currently a Professor in mechanical engineering at the Laboratoire des Technologies Innovantes, University of Picardie Jules Verne, Amiens, France, and a Visiting Professor at the Laboratoire de Réactivité et Chimie des Solides (UPJV). His research interests include additive manufacturing for a wide range of applications including energy storage and electronics.

LOIC DUPONT received the Ph.D. degree in chemistry from the University of Picardie Jules Verne (UPJV), Amiens, France. He is an Expert in electronic microscopy. He is currently a Professor at UPJV as well as the Director of the microscopy platform located at the Hub de l'Énergie. His research interests include additive manufacturing of lithium-ion batteries.

PEDRO CORTES is currently an Associate Professor with the Department of Civil/Enviro nmental and Chemical Engineering Program as well as with the Materials Science and Engineering Program, Youngstown State University. His research work has been funded through the U.S. Department of Transportation, the Department of Defense, NASA, the National Science Foundation, and the Ohio Federal Research Network. He has served twice as a Faculty Fellow of the Wright-Patterson Air Force Base. His research interests include the area of 3D printing, including smart and multifunctional materials, composite structures, and metal-ceramic systems. He has published several articles in the area of composite structures and 3D printing.

CAMEROUN G. SHERRARD has been an Electrical Engineer working on on-demand manufacturing of electronics with the EEE Parts and Failure Analysis Branch, NASA Marshall Space Flight Center, since 2021. She works to develop additively manufactured sensors and circuitry with state-of-the-art electronic printing processes. She worked on electromagnetic contactless coupling system for small spacecraft and loaded polymer-based solid state ultra-capacitors. She has experience with 3D printing, both material extrusion and vat photopolymerization, from prototyping a low-power ocean probe while working with the underwater robotics team at the Georgia Tech Research Institute.

IAN SMALL is currently an Electrical Engineer at the NASA Marshall Space Flight Center and a Subject Matter Expert on additive manufacturing of electronics. He is also the Tech Lead for the On-Demand Manufacturing of Electronics Project and working to develop the equipment, processes, and devices for manufacturing electronics in space and on the lunar/Martian surface. He has substantial experience in additive manufacturing research and development and designing electronics for additive manufacturing processes.

SREEPRASAD T. SREENIVASAN received the B.S. and M.S. degrees in chemistry from Mahatma Gandhi University, India, and the Ph.D. degree in chemistry from the Indian Institute of Technology Madras, India. After completing his Ph.D. degree, he worked as a Postdoctoral Researcher at Kansas State University, USA, and the University of Toledo, USA. He is currently an Assistant Professor of chemistry at the University of Texas at El Paso. Before joining the University of Texas at El Paso, he was a Faculty Member at Clemson University (Research Scientist) and the University of Toledo (Research Assistant Professor). His research interests include materials science and nanotechnology. Especially, he focuses on creating quantum structures, engineering their properties, and applying their modulated properties for security, energy, and sustainability-related applications.

ERIC MACDONALD (Senior Member, IEEE) received the Ph.D. degree in electrical and computer engineering from the University of Texas at Austin, in 2002. He held a Faculty Fellowship at the NASA's Jet Propulsion Laboratory and U.S. Navy Research. He is currently a Professor of mechanical engineering and the Murchison Chair at the University of Texas at El Paso. His research interests include 3D printed multi-functional applications and process monitoring in additive manufacturing with instrumentation and computer vision for improved quality and yield. He is a member of ASME and ASEE and a Registered Professional Engineer, TX, USA. He was awarded the U.S. State Department Fulbright Fellowship in South America.